The Information Carried by Scattered Waves: Near-Field and Non-Asymptotic Regimes

Massimo Franceschetti, Marco D. Migliore, Paolo Minero, and Fulvio Schettino

Abstract—**The question of how much information multiple scattered electromagnetic waves can carry is addressed. The number of spatial degrees of freedom of the field radiated in a two-dimensional setting by a time-harmonic, arbitrary square-integrable current density and in the presence of a random distribution of scattering elements is determined. Using the Born approximation and in the limit of point scatterers, a closed-form expression for the singular value decomposition (SVD) of the field observed on a circular cut separating transmitters and receivers is obtained. It is shown that the active power associated to the kth singular value of the near field in the presence of scatterers external to the cut presents a heavy tail decay as a function of its index, rather than the usual exponential attenuation occurring beyond a critical index term observed in free space. This near field *"information gain"* due to scattering was recently anticipated by Janaswamy using a stochastic source model, it is extended here to arbitrary sources, and it is shown to disappear in the limit of large radiating systems. It is also shown that the same information gain and asymptotic cut-off occurs for the singular values of the field radiating in free space. Collectively, these results show that while the presence of scatterers external to the cut can increase the number of channels that can be exploited for communication by the active power in the near field, they do not change the number of channels associated to the field, nor the asymptotic behavior of the number of degrees of freedom.**

Index Terms—**Degrees of freedom, propagation, scattering, Born approximation, singular value decomposition.**

I. Introduction

THE crossroads of information theory and electromagnetic theory have been explored extensively since the appearance of Shannon's breakthrough paper [1]. Early non-rigorous work of Gabor [2] and Toraldo di Francia [3] has been cast in solid mathematical grounds with the introduction of Slepian's theory of spectral concentration of L^2 functions [4]. It is now well known and rigorously proven [5], [6] that harmonic fields radiated by multiple scattering systems are essentially spatially bandlimited, and hence can be represented on an arbitrary observation domain by a linear combination of an essentially finite number of basis functions, corresponding to the number of degrees of freedom of the field. Recently, this basic result has received renewed attention in the context of multiple-input multiple-output (MIMO) antenna communication systems and wireless networks. In this case, joint space-time encoding and decoding of messages yields parallel spatial channels available for communication and increases the spectral efficiency. The number of available parallel channels is limited by the rank of the communication operator [7], [8], and this is upper bounded by the number of spatial degrees of freedom of the field, as pointed out repeatedly in the literature [9]–[16]. This upper bound holds for arbitrary scattering environments and is independent of stochastic channel modeling assumptions. When multiple users are distributed in a large domain, as in the case of wireless networks, the electromagnetic approach can also be used to bound the information-theoretic capacity of the network in terms of a cut-set integral [17], [18]. This integral represents a suitably normalized measure of the cut separating sources and destinations. The normalization depends on the cut geometry and changes as one moves along the cut [19], but for circular geometries it simply corresponds to the wavelength-normalized size of the circular cut of radius r_s separating transmitters from receivers, see Fig. 1. All of the above results are limited to the asymptotic analysis of large radiating systems, namely $r_s \to \infty$.

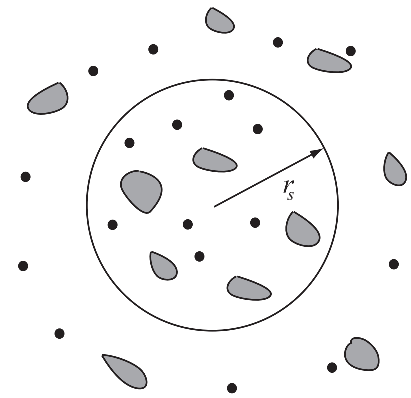

Fig. 1. Cut-set limitation. Transmitting antennas are denoted by black dots inside the circular cut, receiving antennas are denoted by black dots outside the circular cut, scatterers are denoted in grey.

The recent work of Janaswamy [20] examined near field effects for radiating systems of *fixed size*. He focused on the information carried by the active power flux associated to the real part of the Poynting vector. He shows that the number of significant spatial modes increases in the presence of scattering objects outside the cut, due to the interference effect of backscattered waves with the radiated field, that redistributes the reactive power to the modes associated to the active power flux. His result shows that for near field

M. Franceschetti is Department of Electrical and Computer Engineering, University of California, San Diego CA, 92093, USA. Email: massimo@ece.ucsd.edu

P. Minero is with the Electrical Engineering Department, University of Notre Dame, Indiana, IN, Email: pminero@nd.edu.

M. D. Migliore and F. Schettino are with the Microwave Laboratory at the DAEIMI, University of Cassino, 03043 Cassino (FR), Italy. Email: mdmiglio@unicas.it, schettino@unicas.it.

This work was partially supported by the National Science Foundation award CCF-1423648.

communication, the presence of scattering outside the cut can increase the spatial information associated to the active power flux.

In this paper, we present three contributions. First, we consider the *asymptotic regime* of large radiating systems. In this case, we show that even in the presence of scattering and in both near (reactive) and far (radiative) zone, the spatial information of the active power flux is asymptotically limited by the wavelength-normalized size of the cut separating transmitters and receivers. Thus, the presence of scattering outside the cut does not increase the scaling of the spatial information associated to the active power flux. The intuitive explanation is that in the limit of large radiating systems fields are essentially bandlimited functions [6], and the environment can shape their spatial spectrum but it cannot increase their spectral support.

Second, we consider the tail decay of the spatial modes of the near field in the *non-asymptotic regime* of fixed size radiating systems. In this case, we show that in free space near fields exhibit a heavy tail decay in the number of spatial modes, similar to the one of the active power in the presence of scattering. The intuitive explanation is that since near fields radiating in free space carry both active and reactive power, their information content cannot be smaller than the one of the active power after recombination due to backscattering. This result shows that when the receiver is capable of a full field measurement, namely it can measure both the amplitude and the phase of the field, the external scatterers do not provide additional spatial information, even for fixed size systems.

Finally, using the Born approximation, and in the limit of point scatterers, we compute the SVD of the propagation operator for arbitrary square-integrable sources and randomly located scattering elements, and show that Janaswamy's results [20] correspond to the same decomposition, but performed on a different Hilbert space, accounting for a stochastic distribution of sources, and where the norm is expressed in terms of expectation.

The rest of the paper is organized as follows: in Section II we describe different propagation scenarios and present our results, relating them to the previous literature. In section III we give rigorous statements of our results in the form of theorems. In Section IV we discuss numerical examples in some representative cases. In Section V we draw conclusions and discuss possible research directions.

II. Propagation Models

Consider a distribution of time-harmonic source currents located in a circular region S of radius r, radiating an electromagnetic field that is measured on a circle D of radius r_d concentric with S. The number of degrees of freedom of the field is the minimum number of modes that suffice to describe the field on D with an arbitrary level of accuracy, as defined in [5]. The number of degrees of freedom provides an upper bound on the number of channels that are available for communication from S to D and thus on the capacity of any wireless communication system [13], [17].

We distinguish different cases: free space propagation due to arbitrary L^2 sources; propagation in the presence of a random distribution of scattering objects due to a stochastic distribution of sources of bounded second moment; and propagation in the presence of random scattering due to arbitrary L^2 sources.

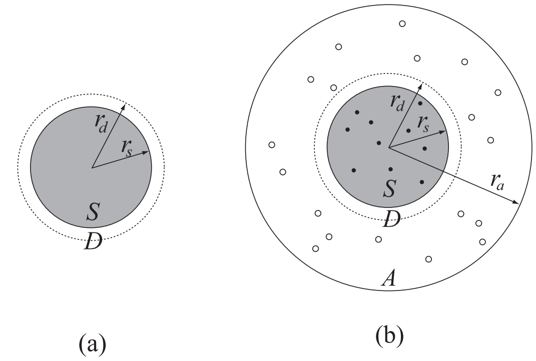

Fig. 2. Part (a): Free space propagation model from an arbitrary distribution of currents inside the disc S. Part (b): Propagation from a random distribution of line currents inside the disc S in the presence of a random distribution of circular scatterers in the annulus A.

A. Free Space Propagation with Arbitrary L^2 Sources

We start considering propagation in the absence of scattering in the two-dimensional cylindrical geometric setting depicted in Fig. 2-(a). This case has been treated extensively in the literature and we review here the basic results useful for our subsequent derivations.

A time-harmonic current density

$$I(\mathbf{r}) = \int_S I(\mathbf{r}')\delta(|\mathbf{r}-\mathbf{r}'|)d\mathbf{r}', \quad \mathbf{r} \in S, \tag{1}$$

is located inside S and is directed along $\hat{z}$, perpendicular to S. The domain outside S is vacuum. The source current is constrained to belong to the Hilbert space $L^2(S)$ of square integrable functions of support S with inner product

$$\langle f, g\rangle_S = \int_S f(\mathbf{r})g^*(\mathbf{r})d\mathbf{r}. \tag{2}$$

and norm

$$\|I\|_S^2 = \int_S |I(\mathbf{r})|^2 d\mathbf{r} < \infty, \tag{3}$$

The electric field radiated by I and observed at $\mathbf{r}_d \in D$ is directed along $\hat{z}$ and is given by

$$E(\mathbf{r}_d) = -\frac{\beta\eta}{4}\int_S I(\mathbf{r})H_0^{(2)}(\beta|\mathbf{r}_d-\mathbf{r}|)d\mathbf{r}, \quad \mathbf{r}_d \in D, \tag{4}$$

where $\beta = 2\pi/\lambda$ is the wavenumber, λ is the radiated wavelength, η is the wave impedance of an electromagnetic wave in vacuum, and $H_0^{(2)}(x)$ is the Hankel function of the second kind and of order 0. The magnetic field is given by

$$H(\mathbf{r}_d) = (j\eta\beta)^{-1}\partial E(\mathbf{r})/\partial r_{|r=r_d}, \quad \mathbf{r}_d \in D. \tag{5}$$

where $\mathbf{r}_d = (r_d, \phi_d)$, $\mathbf{r} = (r, \phi)$.

The integral operator in (4) is compact, so by the spectral decomposition theorem it can be diagonalized. Expanding the integral kernel in terms of the eigenfunctions of the associated self-adjoint operator, we can rewrite (4) as

$$E(\mathbf{r}_d) = \sum_{k=0}^{\infty} \sigma_k \, \langle I, v_k \rangle_S \, u_k(\mathbf{r}_d), \tag{6}$$

where $\{v_k\}$ and $\{u_k\}$ are the right and left singular functions of the operator, respectively, defined as

$$u_k(\mathbf{r}_d) = -\frac{H_k^{(2)}(\beta r_d) e^{jk\phi_d}}{\|H_k^{(2)}(\beta r_d)\|_D}, \tag{7}$$

and

$$v_k(\mathbf{r}) = \frac{J_k(\beta r) \, e^{jk\phi}}{\|J_k(\beta r)\|_S}, \tag{8}$$

and where the real, non-negative coefficients $\{\sigma_k\}$ are the singular values of the operator, defined as

$$\sigma_k = \frac{1}{4} \beta \eta \, \|J_k(\beta r)\|_S \, \|H_k^{(2)}(\beta r_d)\|_D, \tag{9}$$

where $J_k(x)$ denotes the Bessel function of the first kind. A similar expression can be derived for the magnetic field

$$H(\mathbf{r}_d) = \sum_{k=-\infty}^{\infty} \hat{\sigma}_k \, \langle I, v_k \rangle_S \, \hat{u}_k(\mathbf{r}_d), \tag{10}$$

where the left singular functions $\{\hat{u}_k\}$ and the singular values $\{\hat{\sigma}_k\}$ are given by

$$\hat{u}_k(\mathbf{r}_d) = j \frac{H_k^{(2)\prime}(\beta r_d) e^{jk\phi_d}}{\|H_k^{(2)\prime}(\beta r_d)\|_D}, \tag{11}$$

and

$$\hat{\sigma}_k = \frac{1}{4} \beta \, \|J_k(\beta r)\|_S \, \|H_k^{(2)\prime}(\beta r_d)\|_D, \tag{12}$$

respectively. To prove (6) and (10), it suffices to apply the addition theorem for Hankel functions to (4) and (5) such that

$$E(\mathbf{r}_d) = -\frac{\beta \eta}{4} \int_S I(\mathbf{r}) \sum_{k=-\infty}^{\infty} H_k^{(2)}(\beta r_d) J_k(\beta r) e^{jk(\phi_d - \phi)} d\mathbf{r}.$$
$$= -\frac{\beta \eta}{4} \sum_{k=-\infty}^{\infty} \langle I, J_k(\beta r) e^{jk\phi} \rangle_S \, H_k^{(2)}(\beta r_d) e^{jk\phi_d}$$

and, by (5),

$$H(\mathbf{r}_d) = \frac{j\beta}{4} \sum_{k=-\infty}^{\infty} \langle I, J_k(\beta r) e^{jk\phi} \rangle_S \, H_k^{(2)\prime}(\beta r_d) e^{jk\phi_d}.$$

Loosely speaking, the number of degrees of freedom of the radiated field is the number of terms in the series (6) and (10) required to obtain an ϵ-approximation of the field. A basic result in approximation theory [21] states that the magnitude of the nth largest singular value coincides with the norm of the approximation error given by truncating the series to the first n terms. It follows that the number of degrees of freedom can be inferred by the behavior of the singular values as a function of their indexes.

The singular values exhibit a phase transition. They are approximately constant up to a critical value $k \approx \beta r_s$, after which they rapidly decay to zero [5], [17], [18]. When viewed at the scale of r_s, this phase transition becomes more pronounced as r_s increases, and as $r_s \to \infty$ it becomes a step function. The sharpness of the transition ensures that the number of degrees of freedom is an intrinsic feature of the field, that is practically insensitive to the accuracy ϵ of the apparatus with which this is measured. A practical consequence of the phase transition is that an accurate field reconstruction is possible by interpolating only slightly more than βr_s orthonormal functions over D. In other words, the whole information content of the field is essentially given by βr_s real numbers. While the optimal representations (6) and (10) ensure the mininum number of interpolating functions, alternative (e.g. sampling) suboptimal representations can also be used with a slight increase in the number of terms, leading to a possibly redundant field representation.

B. Random Scattering and Stochastic Sources

We now consider the random scattering model considered in [20] and depicted in Fig. 2(b) with the objective of determining whether the phase transition behavior of the singular values still holds in the presence of scattering. Since the scatterers inside D can be treated as equivalent sources, it is sufficient to consider the case of scatterers outside D. Accordingly, a number Q of perfectly conducting cylindrical scatterers, each of radius a, are randomly located in the annular region A delimited by two concentric circles of radii r_d and r_a , that are of the same order of r_s. The region between the observation domain D and the source domain S is vacuum. The scattered field is observed on the circle D of radius r_d circumscribing the source domain S.

The source is a discrete set of N randomly located electric line currents

$$I(\mathbf{r}) = \sum_{n=1}^{N} I_n \delta(|\mathbf{r} - \mathbf{r}_n|), \quad \mathbf{r} \in S \tag{13}$$

where the $\{I_n\}$ are i.i.d. time-harmonic signals of random amplitude and phase. In this case, the input constraint is

$$\mathbb{E}(|I_n|^2) < \infty, \; n \in \{1, \cdots, N\}, \tag{14}$$

where $\mathbb{E}(\cdot)$ denotes the expected value. This corresponds to constraining the sources to belong to the Hilbert space $\bar{L}^2(S)$ with inner product

$$\langle f, g \rangle_S = \mathbb{E}(f g^*), \tag{15}$$

and norm

$$||f||_S = \langle f, f \rangle_S.$$

Comparing the two source models (1) and (13), we notice that (1) only allows a smooth current density in virtue of (3), while (13) consists of space-impulsive currents. The input constraint (14), however, ensures that superdirective effects and unbouded information gains [15], [16] are ruled out when measurements correspond to stochastic averages. Finally, since N is fixed, we can also write the total input constraint

$$\sum_{n=1}^{N} \mathbb{E}(|I_n|^2|) = NP < \infty, \tag{16}$$

that is the discrete counterpart of (3) in the stochastic model.

It follows that the two models correspond to two different Hilbert spaces, where inner products, and hence norms, are governed by (2) and (15) respectively.

Janaswamy's [20] results for the stochastic source model can be viewed in the context of Hilbert spaces as deriving an approximate closed-form expression for the average *real* power carried by the kth singular value of the multiple-scattering propagation operator, where the average is taken with respect to the random amplitude and phase of the line source currents and the random positions of the sources and the scattering objects. He showed that this average power decays as a power law of its index in the near (reactive) zone, and exponentially in the far (radiative) zone. In contrast, he also showed that in free space the decay is always exponential, provided that

$$k > \frac{e\beta r_s}{2}.$$

This critical index value is the same obtained in the dual problem of external sources and scatterers generating a field in a vacuum of radius r_s considered in [22].

Janaswamy then concluded that due to signal interference from scattered paths, part of the reactive power is converted into active power, and the tail of the coefficients representing the real power exhibits a slower decay rate compared to free space conditions. We call this effect the "information gain" for the active power due to scattering in near field conditions.

This result suggests that a phase transition behavior due to the exponential decay of the singular values beyond a critical value of their index may not hold for the real power in the presence of external scatterers. We show that this intuition is incorrect. We point out that the phase transition is a result regarding the step-like behavior of the singular values viewed at an appropriate asymptotic scale, namely $\beta r_s \to \infty$. We show that in this asymptotic regime the heavy tail effect uncovered in [20] disappears. In both free space conditions and in the presence of scattering, the tail of the active power asymptotically vanishes beyond a critical index value of the order of βr_s. This means that in the limit of large radiating systems, there is no information gain due to scattering.

We also point out that for fixed size systems the singular values associated to near fields in free space decay as a power law of their indexes. This shows that for fixed size systems, the information gain for the field is a near field effect, rather than a scattering one.

C. Random Scattering and Arbitrary L^2 Sources

Finally, we consider the random scattering model in the presence of arbitrary L^2 sources subject to (2) and consider the average scattered electric and magnetic fields, where the average is taken with respect to the random position of the scattering objects. We compute the SVD of the propagation operator for the average field using the Born approximation and in the limit of point scatters. From the SVD we compute the active radiated power associated to the kth singular value, showing that in the near (reactive) zone it has a power law behavior as a function of its index, and an exponential behavior in the far (radiative) zone. When sources are assumed to be stochastic, these results recover the ones in [20] and provide a Hilbert space interpretation of the stochastic source model with average squared norm constraint (14).

III. Main results

A. Phase Transition for Large-Scale Systems

In the case of random scattering and stochastic sources, by applying the Born (single scattering) approximation [23] and in the limit of point scatterers, Janaswamy [20] derived an approximate closed-form expression for the average real power associated to the kth singular value of the field, given by

$$\mathrm{Re}(P_k) = \frac{1}{\pi r_d}\,\frac{\beta\eta N P}{8}\,\frac{\|J_k(\beta r)\|_S^2}{\pi r_s^2} \times \left(1 - \mathrm{Re}\left\{\gamma_1\,\mathbb{E}\left(\left(H_k^{(1)}(\beta R)\right)^2\right)\right\}\right), \tag{17}$$

where $k \geq 0$, P is defined in (16),

$$\gamma_j = Q\frac{J_0(\beta a)}{H_0^{(j)}(\beta a)}, \quad j = 1, 2, \tag{18}$$

is a constant that only depends on the size a of the scatterers and their number Q, and

$$\mathbb{E}\left(\left(H_k^{(1)}(\beta R)\right)^2\right) = \frac{2\pi}{\pi(r_a^2 - r_d^2)}\int_{r_d}^{r_a}\left(H_k^{(1)}(\beta r)\right)^2 r dr \tag{19}$$

denotes the expected value of the Hankel function squared with respect to the radial position R of uniformly distributed scatterers inside the annular area of radii r_d and r_a.

By using asymptotic expansions of Bessel functions of large order, he also computed the asymptotic formula[1]

$$\mathrm{Re}(P_k) \sim \frac{P J_0^2(\beta a)\rho_a r_d^2}{|H_0^{(1)}(\beta a)|^2(\pi a)^2}\,\frac{1}{k^4}\left(\frac{r_s}{r_d}\right)^{2k}, \tag{20}$$

as $k \to \infty$. He then noticed that in the near field $r_d \approx r_s$ the exponential term in (20) can be neglected, so that the rate of decay of $\mathrm{Re}(P_k)$ is only polynomial in k. In practice, this means that there is no exponential tail behavior, provided that the measurement of the kth mode occurs sufficiently close to the source.

This result is in sharp contrast with the rate of decay of the real power $\mathrm{Re}(P_k^{(\text{free})})$ carried by the kth singular mode in free-space, that is given by

$$\mathrm{Re}(P_k^{(\text{free})}) \sim \frac{P}{2\pi k(k+1)}\left(\frac{e\beta r_s}{2k}\right)^{2k}, \tag{21}$$

as $k \to \infty$. Since (21) decays exponentially for $k > e\beta r_s/2$, regardless of how close r_s and r_d are, Janaswamy's analysis shows that in the near field external scatterers in D can provide a significant increase of the number of modes associated to the real power, compared to free-space propagation conditions.

Starting from (17), we show that as $r_s \to \infty$ this near field information gain due to scattering disappears, as the singular

[1] Throughout the paper we use the following asymptotic notation. $f(x) \sim g(x) \iff \lim_{x\to x_0} f(x)/g(x) = 1$, $f(x) \in O(g(x))$, as $x \to x_0 \iff \limsup_{x\to x_0} |f(x)/g(x)| < \infty$, $f(x) \in \Theta(g(x))$, as $x \to x_0$, $\iff f(x) \in O(g(x))$ and $g(x) \in O(f(x))$. We also sometime abuse notation and write $O(f(x))$, and $\Theta(f(x))$ to indicate elements of these classes.

modes approach a step function with the same transition point as in the free space case, at a critical index value of the order of βr_s. It follows that the increase in the number of singular modes in the near field does not change known asymptotic limits. The precise statement, proven in Appendix A, is expressed by the following theorem:

Theorem 1: In both the near and radiative zone, there exist an $N_0 = O[\beta r_s \log(\beta r_s)]$ such that for all points on the observation domain, we have

$$\lim_{r_s \to \infty} \sum_{k=N_0}^{\infty} \mathrm{Re}(P_k) = 0. \tag{22}$$

Remark 1: Theorem 1 is the analogous of the one for the electric field in [17, Theorem 3.1], expressed here in the case of the average active power for the random scattering model.

B. Fixed Size Systems, Free Space SVD

In the case of fixed size systems, the free space field carries both active and reactive power and in the near field the singular values exhibit a heavy tail decay as a function of their indexes. The precise statement, proven in Appendix B, is expressed by the following Theorem:

Theorem 2: In the near field, where the exponential term $(r_s/r_d)^k$ can be neglected, the singular values of the electric field in free space are

$$\{\sigma_k^2\} \in \Theta(1/k^3), \quad \text{as } k \to \infty, \tag{23}$$

and the singular values of the magnetic field in free space are

$$\{\hat{\sigma}_k^2\} \in \Theta(1/k) \quad \text{as } k \to \infty. \tag{24}$$

In the radiative zone the singular values exhibit an exponential attenuation as a function of their indexes:

Theorem 3: In the radiative zone, where $(r_s/r_d) < 1$ uniformly in k, the singular values of the electric field in free space are

$$\{\sigma_k^2\} \in O[(r_s/r_d)^{2k}], \quad \text{as } k \to \infty, \tag{25}$$

and the singular values of the magnetic field in free space are

$$\{\hat{\sigma}_k^2\} \in O[(r_s/r_d)^{2k}] \quad \text{as } k \to \infty. \tag{26}$$

Remark 2: Theorems 2 and 3 show that for fixed size systems there is an information gain for the field in free space that is due to the near field measurement. In order to use asymptotic expansions valid for large k in Theorem 2, while neglecting the term $(r_s/r_d)^k$, we must ensure that (r_s/r_d) tends to one *before* the index k tends to infinity. One rigorous way to do this would be to take the limit $r_s/r_d \to 1$ first, so that for any fixed k the term $(r_s/r_d)^k$ can be neglected, and then let $k \to \infty$. This is essentially the approach taken in [20]. Unfortunately, on physical grounds this approach is troublesome. As $r_s/r_d \to 1$ and the receiving domain collapses on the boundary of the radiating system, the field approaches a singularity. It follows that when in the second step we take the limit for $k \to \infty$, we are led to the physical impossibility of determining the decay of the singular values of an infinite field. An alternative approach could be to let $r_s/r_d \to 1$ *while* the index k tends to infinity, and sufficiently fast so that $(r_s/r_d)^k$ does not decay to zero exponentially when $k \to \infty$. Although this can certainly be done mathematically by taking r_s/r_d as a function of the index k, the physical meaning of a field's measurement location that depends on the scaling order at which the singular values are evaluated, also requires clarification.

Despite mathematical sophistications, the physical meaning of the analysis should be clear: we are interested in the tail behavior of the singular values, namely in their behavior for large values of k, but we also want to ensure that for these values the term $(r_s/r_d)^k$ is sufficiently close to one so that it can be neglected. This requires choosing the observation point to be very close to the source. In this *intermediate* regime, we observe a power law decay of the singular values. When k is increased further however, the approximation does not hold anymore and the exponential regime of Theorem 3 is entered. Of course, at this point we may choose r_s even closer to r_d, and "push" the exponential regime further away, and so on. In practice, in order to appreciate the near field information gain, one needs to be sufficiently close to the field's singular point $r_s = r_d$ to combat the exponential decay of the singular values. In short: the information gain for the field in free space is a pure near field effect.

C. Fixed Size Systems, SVD with Random Scattering

We now compute an approximate SVD of the field in the presence of random scattering. We first consider the case of arbitrary L^2 sources defined by (1) and subject to (3), and then the case of stochastic $\bar{L}^2$ sources defined by (13) and subject to (14). In the latter case, we also show that when computing the average power from the SVD, our results coincide with the ones of [20]. This provides an interpretation of this work in terms of spectral decomposition of the propagation operator in $\bar{L}^2$.

We divide the total field into a direct component and a scattered component

$$(E, H) = (E_i, H_i) + (E_s, H_s). \tag{27}$$

The SVD of the direct component (E_i, H_i) is the one given in Section II-A. The scattered component (E_s, H_s) is given by the current density induced on the surface of the scattering cylinders. To obtain the SVD of this latter term we make the following approximations, numerically validated in [20]:

Assumption 1 (Born approximation): The density of the scatterers is low enough such that multiple scattering is negligible.

Assumption 2 (Point scatterers): The scatterers are small enough that only the first term of the Fourier series representation of the currents induced on their surface is significant.

Using these approximations, in Appendix C we compute the SVD of the average scattered electric field, for uniformly distributed scatters inside the annular area of radii r_d and r_a, that is

$$\mathbb{E}\left(E_s(\mathbf{r}_d)\right) = \sum_{k=-\infty}^{\infty} \sigma_k^{(s)} \langle I, v_k\rangle_S \, u_k^{(s)}(\mathbf{r}_d), \tag{28}$$

where v_k is given by (8),

$$u_k^{(s)}(\mathbf{r}_d) = \frac{w_k(r_d)e^{jk\phi_d}}{\|w_k(r_d)\|_D}, \tag{29}$$

and

$$\sigma_k^{(s)} = \frac{1}{4}\eta\beta \, \|J_k(\beta r)\|_S \, \|w_k(r_d)\|_D \tag{30}$$

with

$$\begin{aligned} w_k(r_d) &= \gamma_2 \frac{2\pi}{\pi(r_a^2 - r_d^2)} \int_{r_d}^{r_a} \left(H_k^{(2)}(\beta r)\right)^2 r dr \; J_k(\beta r_d). \\ &= \gamma_2 \; \mathbb{E}\Big(\left(H_k^{(2)}(\beta R)\right)^2\Big) \; J_k(\beta r_d). \end{aligned} \tag{31}$$

In (31), γ_2 is defined as in (18), and the expectation is given by (19). Notice that the SVD of the incident field (6) and the one of the average scattered field (28) differ only in the way the set of functions $\{u_k\}$ and $\{u_k^{(s)}\}$ are defined. Both u_k and $\{u_k^{(s)}\}$ are proportional to a basic solution of the Helmholtz equation in cylindrical coordinates, but the random scatterers affect the proportionality constant, which in (31) depends on the average of the Hankel squared over a uniform radial distribution in A.

Similarly, we obtain the SVD of the average scattered magnetic field

$$\mathbb{E}\left(H_s(\mathbf{r}_d)\right) = \sum_{k=-\infty}^{\infty} \hat{\sigma}_k^{(s)} \langle I, v_k\rangle_S \, \hat{u}_k^{(s)}(\mathbf{r}_d), \tag{32}$$

where

$$\hat{u}_k^{(s)}(\mathbf{r}_d) = \frac{\hat{w}_k(r_d)e^{jk\phi_d}}{\|\hat{w}_k(r_d)\|_D}, \tag{33}$$

$$\hat{\sigma}_k^{(s)} = \frac{1}{4}\beta \, \|J_k(\beta r)\|_S \, \|\hat{w}_k(r_d)\|_D \tag{34}$$

with

$$\hat{w}_k(r_d) = -j \; \gamma_2 \; \mathbb{E}\Big(\left(H_k^{(2)}(\beta R)\right)^2\Big) \; J_k'(\beta r_d). \tag{35}$$

Notice that, consistently with (5), (32) is obtained from (28) by differentiation of (31) over the radial distance , which yields (35).

From the SVD, we obtain the analogous of Theorem 2 and 3 in the case of random scattering:

Theorem 4: In the near field, where the exponential term $(r_s/r_d)^k$ can be neglected, the singular values of the electric field in the presence of random scattering are

$$\{(\sigma_k^{(s)})^2\} \in \Theta(1/k^7), \quad \text{as } k \to \infty, \tag{36}$$

and the singular values of the magnetic field in the presence of random scattering are

$$\{(\hat{\sigma}_k^{(s)})^2\} \in \Theta(1/k^5) \quad \text{as } k \to \infty. \tag{37}$$

In the radiative zone field the singular values exhibit an exponential attenuation as a function of their indexes:

Theorem 5: In the radiative zone, where $(r_s/r_d) < 1$, uniformly in k, the singular values of the electric field in the presence of random scattering are

$$\{\sigma_k^2\} \in O[(r_s/r_d)^{2k}], \quad \text{as } k \to \infty, \tag{38}$$

and the singular values of the magnetic field in the presence of random scattering are

$$\{\hat{\sigma}_k^2\} \in O[(r_s/r_d)^{2k}] \quad \text{as } k \to \infty. \tag{39}$$

Remark 3: Theorems 4 and 5, combined with Theorems 2 and 3, show that for fixed size systems there is an information gain for both the free space field and for the scattered field that is a pure near field measurement, occurring when $r_s \approx r_d$. In contrast, from (20) and (21) it follows that the near field information gain for the real power occurs only in the presence of scattering. The asymptotic behaviors of the singular values of the electric and magnetic fields for fixed size systems with scattering are different from the behavior of the real power in (20) because this involves performing an average over the product of the two fields. When this average is carried out, the two results match.

D. Expected Power with Random Scattering

From the SVD, we now compute the expected power associated to each singular value in the presence of scattering. The complex power per unit length along $\hat{z}$ is given by

$$\begin{aligned} P(\mathbf{r}_d) = -\frac{1}{2}\int_0^{2\pi} r_d \big(E_i(\mathbf{r}_d) + E_s(\mathbf{r}_d)\big) \\ \times \big(H_i(\mathbf{r}_d) + H_s(\mathbf{r}_d)\big)^* d\phi_d, \end{aligned} \tag{40}$$

Taking the expectation with respect to the random position of the scatterers and substituting (6), (10), (28), and (32) into (40), the expected complex power at a point $\mathbf{r}_d \in D$ can be decomposed as follows

$$\begin{aligned} \mathbb{E}[P(\mathbf{r}_d)] &= \sum_{k=-\infty}^{\infty} P_k(r_d) \\ &= \sum_{k=-\infty}^{\infty} P_k^{ii}(r_d) + P_k^{ss}(r_d) + P_k^{is}(r_d) + P_k^{si}(r_d), \end{aligned} \tag{41}$$

where the four terms in the summation (41) have superscripts indicating which field components—incident (i) or scattered (s)—are combined to obtain the corresponding power term. $P_k^{is}(r_d)$, for instance, is the power term due to the combination of the kth mode in the incident electric field's expansion (6) and the kth mode in the scattered magnetic field's expansion (32), i.e.,

$$\begin{aligned} P_k^{ii}(r_d) = -\frac{1}{2}\int_0^{2\pi} \sigma_k \; \hat{\sigma}_k \; |\langle I, v_k\rangle_S|^2 \\ \times u_k(\mathbf{r}_d) \; \hat{u}_k^*(\mathbf{r}_d) \; r_d \; d\phi_d. \end{aligned} \tag{42}$$

Making use of the SVD's for the incident and scattered fields we obtain the following expressions

$$P_k^{ii}(r_d) = -j\alpha H_k^{(2)}(\beta r_d) \; H_k^{(1)\prime}(\beta r_d), \tag{43}$$

$$P_k^{ss}(r_d) = j\alpha \left| \gamma_2 \, \mathbb{E}\Big(\big(H_k^{(2)}(\beta R) \big)^2 \Big) \right|^2 J_k(\beta r_d) \; J_k'(\beta r_d), \tag{44}$$

$$P_k^{is}(r_d) = j\alpha \left(\gamma_2 \, \mathbb{E}\Big(\big(H_k^{(2)}(\beta R) \big)^2 \Big) \right)^* H_k^{(2)}(\beta r_d) J_k'(\beta r_d) \tag{45}$$

$$P_k^{si}(r_d) = j\alpha \; \gamma_2 \, \mathbb{E}\Big(\big(H_k^{(2)}(\beta R) \big)^2 \Big) \; J_k(\beta r_d) \; H_k^{(1)\prime}(\beta r_d), \tag{46}$$

where in (43)–(46) we define

$$\alpha = \frac{\pi r_d}{2} \frac{\beta^2 \eta}{8} \; \| J_k(\beta r) \|_S^2 \; |\langle I, v_k \rangle_S|^2. \tag{47}$$

The real power can be expressed as a series of the real parts of (43)–(46). We analyze each term separately. First,

$$\begin{aligned} \mathrm{Re}\{P_k^{ii}(r_d)\} &= \alpha \, \mathrm{Im}\{ H_k^{(2)}(\beta r_d) \; H_k^{(1)\prime}(\beta r_d) \} \\ &= -\frac{\beta \eta}{8} \; \| J_k(\beta r) \|_S^2 \; |\langle I, v_k \rangle_S|^2, \end{aligned} \tag{48}$$

where the last equality uses the Wronskian property of Bessel's functions

$$\begin{aligned} &\mathrm{Im}\big\{ H_k^{(2)}(\beta r_d) \; H_k^{(1)\prime}(\beta r_d) \big\} \\ &\quad = Y_k(\beta r_d) J_k'(\beta r_d) - Y_k'(\beta r_d) J_k(\beta r_d) \\ &\quad = -\frac{2}{\pi \beta r_d}. \end{aligned} \tag{49}$$

Next, we have

$$\mathrm{Re}\big\{ P_k^{ss}(r_d) \big\} = 0 \tag{50}$$

since $P_k^{ss}(r_d)$ only comprises of reactive power. Finally,

$$\begin{aligned} &\mathrm{Re}\big\{ P_k^{is}(r_d) + P_k^{si}(r_d) \big\} \\ &= -\alpha \, \mathrm{Im} \Big\{ \left(\gamma_2 \, \mathbb{E}\Big(\big(H_k^{(2)}(\beta R) \big)^2 \Big) \right)^* H_k^{(2)}(\beta r_d) J_k'(\beta r_d) \\ &\qquad + \gamma_2 \, \mathbb{E}\Big(\big(H_k^{(2)}(\beta R) \big)^2 \Big) \; J_k(\beta r_d) \; H_k^{(1)\prime}(\beta r_d) \Big\} \\ &= \frac{\beta \eta}{8} \| J_k(\beta r) \|_S^2 |\langle I, v_k \rangle_S|^2 \\ &\quad \times \mathrm{Re} \left\{ \gamma_2 \mathbb{E}\Big(\big(H_k^{(2)}(\beta R) \big)^2 \Big) \right\}, \end{aligned} \tag{51}$$

where the last equality follows from the fact that for every $z \in \mathbb{C}$

$$\begin{aligned} &\mathrm{Im}\big\{ z^* H_k^{(2)}(\beta r_d) J_k'(\beta r_d) + z J_k(\beta r_d) H_k^{(1)\prime}(\beta r_d) \big\} \\ &\quad = \mathrm{Re}\{z\} \big(Y_k(\beta r_d) J_k'(\beta r_d) - Y_k'(\beta r_d) J_k(\beta r_d) \big) \\ &\quad = -\mathrm{Re}\{z\} \frac{2}{\pi \beta r_d}. \end{aligned} \tag{52}$$

By combining (41), (48), (50), and (51), it follows that

$$\begin{aligned} \mathrm{Re}\{P_k(r_d)\} = &-\frac{\beta \eta}{8} \| J_k(\beta r) \|_S^2 \; |\langle I, v_k \rangle_S|^2 \\ &\times \left(1 - \mathrm{Re} \left\{ \gamma_2 \, \mathbb{E}\Big(\big(H_k^{(2)}(\beta R) \big)^2 \Big) \right\} \right). \end{aligned} \tag{53}$$

We also compute the reactive power in free space

$$\begin{aligned} \mathrm{Im}\{P_k^{ii}(r_d)\} &= -\alpha \, \mathrm{Re}\{ H_k^{(2)}(\beta r_d) \; H_k^{(1)\prime}(\beta r_d) \} \\ &= -\alpha (J_k(\beta r_d) J_k'(\beta r_d) + Y_k(\beta r_d) Y_k'(\beta r_d)), \end{aligned} \tag{54}$$

whose asymptotic limit for fixed argument and large orders is

$$\mathrm{Im}\{P_k^{ii}(r_d)\} \sim \frac{\beta \eta}{8} \; |\langle I, v_k \rangle_S|^2 \frac{r_s^2}{k(k+1)} \left(\frac{r_s}{r_d} \right)^{2k}. \tag{55}$$

E. Expected Real Power with Stochastic Sources

We now show that the results in [20] are recovered by the SVD result derived in Sec. III-D, assuming stochastic sources and working in Hilbert space $\bar{L}^2$, where the scalar product is given by (15). Assume that I is as in (13). Then, by (15) and the independence of the sources, we have

$$\begin{aligned} |\langle I, v_k \rangle_S|^2 = \mathbb{E} \Bigg(&\sum_{n=1}^{N} \sum_{m=1}^{N} |I_n| |I_m| \\ &e^{j(\angle I_n - \angle I_m)} v_k^*(\mathbf{r}_n) v_k(\mathbf{r}_m) \Bigg). \end{aligned} \tag{56}$$

Averaging the right hand side of (56) over the phases $\{\angle I_n\}$ yields

$$\mathbb{E}_{\angle I_n}\big(|\langle I, v_k \rangle_S|^2 \big) = \sum_{n=1}^{N} |I_n|^2 |v_k(\mathbf{r}_n)|^2. \tag{57}$$

Then, after averaging (57) over the random locations $\{\mathbf{r}_n\}$, we obtain

$$\mathbb{E}_{\angle I_n, \mathbf{r}_n}\big(|\langle I, v_k \rangle_S|^2 \big) = \sum_{n=1}^{N} |I_n|^2 \frac{1}{\pi r_s^2}. \tag{58}$$

Finally, by (16) and by averaging over $|I_n|^2$, we obtain

$$\mathbb{E}\big(|\langle I, v_k \rangle_S|^2 \big) = \frac{NP}{\pi r_s^2}, \tag{59}$$

where the expectation is with respect to the source's magnitudes, phases, and location in S. By combining (53) with (59) and making use of the fact that for every complex number $z_1 \; z_2$

$$\mathrm{Re}\{z_1 z_2\} = \mathrm{Re}\{z_1^* z_2^*\} \tag{60}$$

we have

$$\begin{aligned} \mathrm{Re}\{P_k\} = &-\frac{\beta \eta N P}{8} \frac{\| J_k(\beta r) \|_S^2}{\pi r_s^2} \\ &\times \left(1 - \mathrm{Re} \left\{ \gamma_1 \mathbb{E}\Big(\big(H_k^{(1)}(\beta R) \big)^2 \Big) \right\} \right). \end{aligned} \tag{61}$$

The result (61) should be compared with (53). The difference is due to the additional expectation over the sources, required by the scalar product in $\bar{L}^2$. Finally, (17) is recovered by dividing (61) by the factor $-\pi r_d$ that has been accounted as a constant in [20].

IV. Numerical examples

We now provide some examples to visualize the physical meaning of our mathematical results. In all examples distances are in wavelengths and the numerical values are chosen close to the ones [20] for comparison. Fig. 3 shows the information gain unveiled by Janaswamy [20], namely the increase in the tail of the active power in the presence of scattering. The plot refers to the case when sources are arbitrary functions in L^2, while in the case of [20] sources are stochastic functions

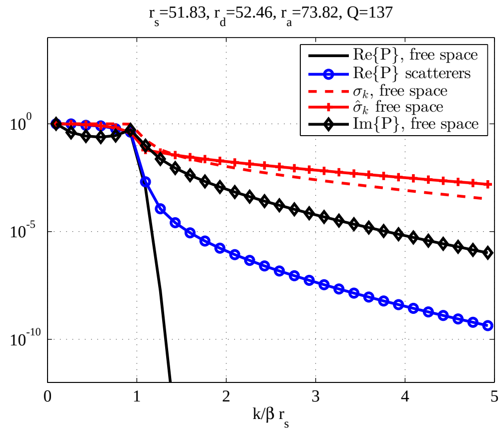

Fig. 3. Active power in free space (48), active power in the presence of scatterers (53), reactive power in free space (54), singular values σ_k of the electric field in free space (9), and singular values $\hat{\sigma}_k$ of the magnetic field in free space (12) versus the normalized mode number $k/\beta r_s$.

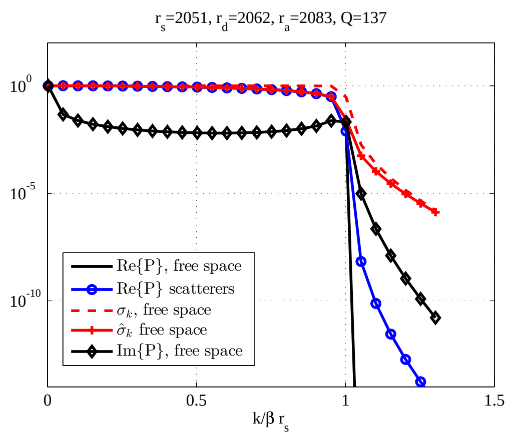

Fig. 4. Active power in free space (48), active power in the presence of scatterers (53), reactive power in free space (54), singular values σ_k of the electric field in the free space (9), and singular values $\hat{\sigma}_k$ of the magnetic field in free space (12) versus the normalized mode number $k/\beta r_s$, for a large radiating system.

in $\bar{L}^2$, but the effect of increasing the number of significant modes associated to the active power, compared to free-space conditions is the same. From the plot it is evident that in free space the active power decays exponentially as a function of its index, while in the presence of scattering it presents a heavy-tail attenuation. The figure also shows the heavy-tail decay of the singular values of the field in free space (Theorem 2) and of the reactive power in free space. Due to scattering, part of the reactive power is converted into active power and this is responsible for the information gain effect. These results show that while scattering can increase the number of channels that can be used for communication by the active power, this cannot be larger than the number of channels associated to the free space field, that carries both active and reactive power.

Fig. 4 shows that the information gain effect disappears for large radiating systems. From the plot it is evident that a much more pronounced step-like behavior arises for a large radiating system around a critical index value of the order of βr_s, for both the power (Theorem 1) and the field (Remark 1). These

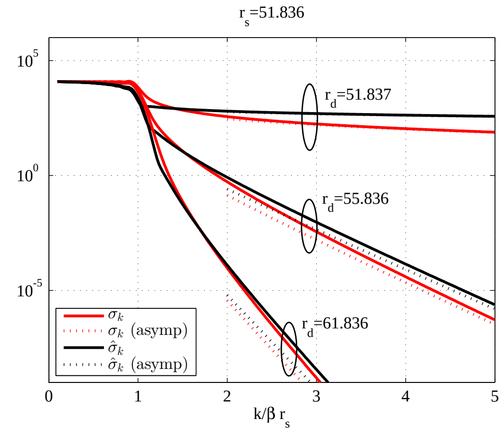

Fig. 5. Singular values for electric (9) and magnetic (12) fields in free space. The asymptotic values correspond to (86) and (89). In the near field regime the heavy tail is more pronounced, while it transitions to an exponential tail in the radiative zone.

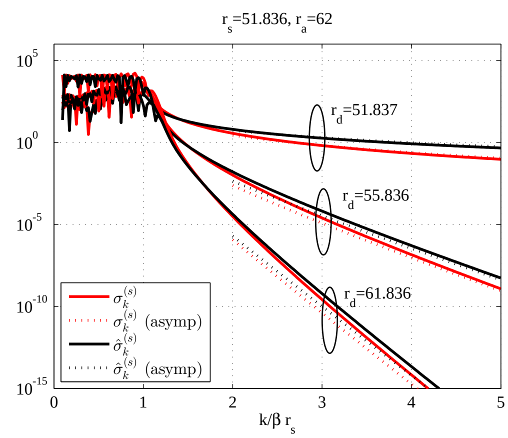

Fig. 6. Singular values for electric (30) and magnetic (34) fields in the presence of scattering. The asymptotic values correspond to (106) and (107). In the near field regime the heavy tail is more pronounced, while it transitions to an exponential tail in the radiative zone.

results show that the presence of scatterers does not change the scaling behavior of the number of degrees of freedom.

Fig. 5 and Fig. 6 take a closer look at the singular values of the field in free space and in the presence of scattering. From the plots it is evident that a heavy-tail behavior of the singular values occurs in the near field, where $r_s/r_d \approx 1$ (Theorems 2 and 4). On the other hand, as r_d increases an exponential tail behavior becomes dominant (Theorems 3 and 5). These results show that there is no information gain due to scattering for the field. Since both in the presence or absence of scattering a heavy tail occurs in the near field, there is an information gain for the field due to the near field measurement. This information gain disappears in the scaling limit of large systems, as shown in Fig. 4.

V. Conclusion

We have examined the information gain, in terms of number of spatial channels available for communication, due to near field and scattering effects. For electromagnetic fields, the information gain is purely a near field effect, occurring in the presence or absence of scattering and manifests itself in terms of a power law decay of the singular values as a function of their indexes, when the receiver is very close to the source. On the other hand, for the active power the information gain in the near field occurs only in the presence of scattering, that allows conversion of part of the reactive power into active power.

By interpreting the singular values of the field's decomposition as communication channels, our results indicate that systems of fixed size communicating in the near field can provide additional multiplexing capabilities compared to their radiative zone counterparts. However, we have also shown that the information gain for both the fields and the active power tends to disappear as the size of the communication system is increased. For large antenna arrays or distributed wireless networks, the number of parallel channels available for communication concentrates at the scale of the circular cut-set separating transmitters and receivers, normalized by the wavelength of transmission. This result is independent of scattering, reactive, or radiative zone assumptions.

Finally, we point out that when our results are applied in the context of remote sensing, illuminating a spatial scene by a time-harmonic source, they quantify the information gain corresponding to the increased resolution available in the image due to scattering and near field effects.

Appendix A
Proof of Theorem 1

From (17) it follows that

$$\mathrm{Re}(P_k) \leq \frac{1}{\pi r_d} \frac{\beta\eta NP}{8} \frac{\|J_k(\beta r)\|_S^2}{\pi r_s^2} \times \Big(1 + \Big|\gamma_1 \, \mathbb{E}\Big(\big(H_k^{(1)}(\beta R)\big)^2\Big)\Big|\Big), \tag{62}$$

The norm and expectation in (17) can be can be evaluated using the identity [20], [24], [25]

$$\begin{aligned} F_k(r; Z) &:= \int_0^r x Z_k^2(\beta x) dx \\ &= \frac{r^2}{2}(Z_k^2(\beta r) - Z_{k-1}(\beta r) Z_{k+1}(\beta r)) \\ &= \frac{1}{2\beta^2}(k^2 Z_k'^2(\beta r) - (k^2 - \beta^2 r^2) Z_k^2(\beta r)) \end{aligned} \tag{63}$$

where Z_k is any integer valued Bessel function. It follows from (63) that if Z_k is real-valued, then

$$F_k(r; Z) \leq \frac{k^2}{2\beta^2} Z_k'^2(\beta r)$$

for every $k \geq \beta x$. Hence,

$$\|J_k(\beta r)\|_S^2 = 2\pi F_k(r_s; J) \leq \frac{k^2 \pi}{\beta^2} J_k'^2(\beta r_s) \tag{64}$$

for every $k \geq \beta r_s$. Similarly, for every $k \geq \beta r_a$

$$\begin{aligned} \left|\int_{r_d}^{r_a} \big(H_k^{(1)}(\beta r)\big)^2 r dr\right| &\leq \int_{r_d}^{r_a} \big|H_k^{(1)}(\beta r)\big|^2 r dr \\ &= \int_A \Big(|J_k(\mathbf{r})|^2 + |Y_k(\mathbf{r})|^2\Big) d\mathbf{r} \\ &= 2\pi\Big(F_k(r_a; J) + F_k(r_a; Y) \\ &\quad - F_k(r_d; J) - F_k(r_d; Y)\Big) \\ &\leq 2\pi\Big(F_k(r_a; J) + F_k(r_a; Y)\Big) \\ &= \frac{k^2\pi}{\beta^2}\Big(J_k'^2(\beta r_a) + Y_k'^2(\beta r_a)\Big) \\ &= \frac{k^2\pi}{\beta^2} |H_k^{(1)'}(\beta r_a)|^2 \end{aligned} \tag{65}$$

By combining (62) with (64) and (65), it follows that for every $k \geq \beta r_a$

$$\mathrm{Re}(P_k) \leq \frac{1}{\pi r_d} \frac{\beta\eta NP}{8} \frac{k^2}{\beta^2 r_s^2} J_k'^2(\beta r_s) \times \frac{2|\gamma_1|}{(r_a^2 - r_d^2)} \frac{k^2\pi}{\beta^2} |H_k'^{(1)}(\beta r_a)|^2. \tag{66}$$

Next, we use Olver's uniform asymptotic expansions for Bessel functions [26] [27] to bound the right-hand side of (66). It is established that while the derivative of the Hankel function $|H_k^{(1)'}(\beta r_a)|$ is exponentially increasing in k, the derivative of the Bessel function $|J_k'(\beta r_s)|$ is exponentially decreasing in k. By studying the rate of growth and decay of the two functions, we conclude that (66) decreases exponentially to zero as k approaches infinity.

Let z_1 denote the ratio between the argument and the order of $J_k'(\beta r_s)$, i.e. $z_1 = \frac{\beta r_s}{k}$. Identity (5.10) of [27] and the triangle inequality yield, for $0 < z_1 \leq 1$,

$$\begin{aligned} |J_k'(kz_1)| \leq \frac{2}{k^{2/3} z_1} \left(\frac{1 - z_1^2}{4\zeta(z_1)}\right)^{1/4} \Big[&\frac{\mathrm{Ai}\big(k^{2/3}\zeta(z_1)\big)}{k^{2/3}} \\ &+ \Big|\mathrm{Ai}'\big(k^{2/3}\zeta(z_1)\big)\Big| + |\eta_1(k, z_1)| \\ &+ \frac{|\epsilon_1(k, z_1)|}{k^{2/3}}\Big], \end{aligned} \tag{67}$$

wherein Ai denotes the Airy function, for $0 < z_1 \leq 1$ the function $\zeta(z_1)$ is defined as,

$$\begin{aligned} \frac{2}{3}\zeta^{3/2}(z_1) &= \int_{z_1}^1 \frac{\sqrt{1 - u^2}}{u} du \\ &= \log\left(\frac{1 + \sqrt{1 - z_1^2}}{z_1}\right) - \sqrt{1 - z_1^2}, \end{aligned} \tag{68}$$

and $|\epsilon(k, z_1)|$ and $|\eta(k, z_1)|$ are subject to the following bounds [27, Section 5]:

$$|\epsilon_1(k, z_1)| \leq k^{-1} |\mathrm{Ai}'\big(k^{2/3}\zeta(z_1)\big)|, \tag{69}$$

$$|\eta_1(k, z_1)| \leq k^{-1} \mathrm{Ai}\big(k^{2/3}\zeta(z_1)\big). \tag{70}$$

Substituting (69) and (70) into (67), and using $\mathrm{Ai}(x)/|\mathrm{Ai}'(x)| \leq 2$, which holds for all $x \geq 0$ [27, page 11], we obtain that, for $0 < z_1 \leq 1$,

$$|J_k'(kz_1)| \leq \frac{14}{k^{2/3} z_1} \left(\frac{1 - z_1^2}{4\zeta(z_1)}\right)^{1/4} \big|\mathrm{Ai}'(k^{2/3}\zeta(z_1))\big|. \tag{71}$$

Equation (71) provides a bound (uniform in $0 < z_1 \leq 1$) for $|J_k'(kz_1)|$ in terms of the derivative of the Airy function.

Similarly, we can derive a bound for the derivative of the Hankel function. Let z_2 denote the ratio between the argument and the order of $H_k^{(2)'}(\beta r_a)$, i.e. $z_2 = \frac{\beta r_a}{k}$. Similarly to (71), it is possible to show that

$$|Y_k'(kz_2)| \le \frac{14}{k^{2/3}\ z_2}\left(\frac{1-z_2^2}{4\zeta(z_2)}\right)^{1/4} \mathrm{Bi}'(k^{2/3}\zeta(z_2)), \quad (72)$$

where Bi denotes the Airy function of the second kind. Since $\left|H_k^{(2)\prime}(kz_2)\right| \le 2\big(|J_k'(kz_2)| + |Y_k'(kz_2)|\big)$, combining (71) with (72), we obtain

$$\left|H_k^{(2)\prime}(kz_2)\right| \le \frac{28}{k^{2/3}\ z_2}\left(\frac{1-z_2^2}{4\zeta(z_2)}\right)^{1/4} \times \left(\left|\mathrm{Ai}'(k^{2/3}\zeta(z_2))\right| + \mathrm{Bi}'(k^{2/3}\zeta(z_2))\right). \quad (73)$$

The derivatives of the Airy functions can be bounded for $k^{2/3}\zeta(z_2) \ge 1$ as follows [28, page 394]:

$$\begin{aligned} |\mathrm{Ai}'(k^{2/3}\zeta(z_2))| &\le k^{1/6}\zeta^{1/4}(z_2)e^{-\frac{2}{3}k\zeta^{3/2}(z_2)}, \\ |\mathrm{Bi}'(k^{2/3}\zeta(z_2))| &\le k^{1/6}\zeta^{1/4}(z_2)e^{+\frac{2}{3}k\zeta^{3/2}(z_2)}. \end{aligned} \quad (74)$$

By (68), we notice that $\zeta(z_2)$ is a decreasing function of z_2, which tends to infinity as $z_2 \to 0^+$ and is 0 when $z_2 = 1$. Hence, the condition $k^{2/3}\zeta(z_2) \ge 1$, which is required for (74) to hold, is not satisfied when z_2 is close to 1. Moreover, notice that $\zeta(z_2) < \zeta(z_1)$, since $|z_2| > |z_1|$ for any $r_a > r_s$. It follows that choosing $k \ge \beta r_a \log r_a$ ensures that both $k^{2/3}\zeta(z_2) \ge 1$ and $k^{2/3}\zeta(z_1) \ge 1$ hold for r_a and r_s large.

Substituting (74) into (71) and (73), it follows that, for $k \ge \beta r_a \log r_a$,

$$\left|H_k^{(2)\prime}(\beta r_a)\right| = O\left(\frac{(1-z_2^2)^{1/4}}{k^{1/2}\ z_2} e^{+\frac{2}{3}k\zeta^{3/2}(z_2)}\right), \quad (75)$$

$$|J_k'(\beta r_s)| = O\left(\frac{(1-z_1^2)^{1/4}}{k^{1/2}\ z_1} e^{-\frac{2}{3}k\zeta^{3/2}(z_1)}\right), \quad (76)$$

as $r_a, r_s \to \infty$. Since $\zeta(z_2) < \zeta(z_1)$ for any $r_a > r_s$, the rate of growth of the exponential in (75) is smaller than the rate of decay of the exponential in (76). Using (75), (76), and the fact that $(1-z_2^2)^{1/4}(1-z_1^2)^{1/4}/(kz_2z_1) \le k$ for $k > \beta r_a \log r_a$, we obtain that for $k > \beta r_a \log r_a$,

$$|J_k'(\beta r_s)|\left|H_k^{(2)\prime}(\beta r_a)\right| = O\left(ke^{-\frac{2}{3}k(\zeta^{3/2}(z_1)-\zeta^{3/2}(z_2))}\right) \quad (77)$$

as $r_s \to \infty$.

Let us focus on the exponent at the right-hand side of (77). By (68),

$$\begin{aligned} &-k\left(\frac{2}{3}\zeta^{3/2}(z_1) - \frac{2}{3}\zeta^{3/2}(z_2)\right) \\ &= -k\int_{z_1}^{z_2} \frac{\sqrt{1-u^2}}{u}du \\ &\le -k\int_{z_1}^{z_2}\left(\frac{1}{u}-1\right)du \\ &= -k\log\left(\frac{z_2}{z_1}\right) + k(z_2-z_1), \\ &= -k\log\left(\frac{r_a}{r_s}\right) + \beta(r_a - r_s), \end{aligned} \quad (78)$$

where the inequality follows from $\sqrt{1-u^2} \ge 1-u$, for all $u \in [0,1]$. Substituting (78) into (77) it follows that, for all $r_a > r_s$ and for all $k \ge \beta r_a \log r_a$,

$$|J_k'(\beta r_s)|\left|H_k^{(2)\prime}(\beta r_a)\right| = O\left(ke^{-k\ \log(r_a/r_s)}\right), \quad (79)$$

as $r_s \to \infty$. Since r_a is of the same order of r_s, we can assume that $r_a = \alpha r_s$ for some $\alpha > 1$, and (79) becomes

$$|J_k'(\beta r_s)|\left|H_k^{(2)\prime}(\beta r_a)\right| = O\left(ke^{-k\ \log\alpha}\right), \quad (80)$$

as $r_s \to \infty$.

We now go back to (66) and notice that we can group all factors except $J_k'^2(\beta r_s)$ and $\left|H_k^{(2)\prime}(\beta r_a)\right|^2$ into a term of the order of $O(r_s^\nu)$ for some $\nu \ge 0$ as $r_s \to \infty$. It follows that letting $N_0 = \beta r_a \log r_a$ and using the bound (80), which is uniform in $k \ge N_0 > \beta r_s$, there exists a uniform constant C, such that as $r_s \to \infty$, we have

$$\begin{aligned} \sum_{k=N_0}^{\infty} \mathrm{Re}(P_k) &\le r_s^\nu \sum_{k=N_0}^{\infty} Ce^{-2k\log\alpha} \\ &= r_s^\nu \frac{Ce^{-N_0 2\log\alpha}}{1-e^{-2\log\alpha}} \\ &\le C\frac{r_s^\nu}{\alpha^{\beta r_s}} \\ &\to 0, \end{aligned} \quad (81)$$

which concludes the proof.

Appendix B
Proof of Theorems 2 and 3

For fixed argument and large orders with $k > z$ [24, §10.19]

$$Y_k(z) \sim -jH_k^{(1)}(z) \sim jH_k^{(2)}(z) \sim -\sqrt{\frac{2}{\pi k}}\left(\frac{ez}{2k}\right)^{-k} \quad (82)$$

and

$$J_k(z) \sim \frac{1}{\sqrt{2\pi k}}\left(\frac{ez}{2k}\right)^k \quad (83)$$

From (82) it follows that

$$\begin{aligned} \|H_k^{(2)}(\beta r_d)\|_D^2 &= 2\pi r_d |H_k^{(2)}(\beta r_d)|^2 \\ &\sim \frac{4r_d}{k}\left(\frac{e\beta r_d}{2k}\right)^{-2k}, \end{aligned} \quad (84)$$

while combining (63) and (83) yields the asymptotic form

$$\|J_k(\beta r)\|_S^2 \sim \frac{r_s^2}{2k(k+1)}\left(\frac{e\beta r_s}{2k}\right)^{2k} \quad (85)$$

as $k \to \infty$. By combining (9), (84), and (85), we obtain

$$\sigma_k^2 \sim \frac{1}{8}\beta^2\eta^2\ \frac{r_s^2 r_d}{k^2(k+1)}\left(\frac{r_s}{r_d}\right)^{2k}. \quad (86)$$

Neglecting the exponential term $(r_s/r_d)^k$, we also have

$$\sigma_k^2 \sim \frac{\beta^2\eta^2 r_s^3}{8k^3}. \quad (87)$$

Similarly,

$$\begin{aligned} \|H_k^{(2)\prime}(\beta r_d)\|_D^2 &= 2\pi r_d |H_k^{(2)\prime}(\beta r_d)|^2 \\ &\sim \frac{r_d}{k+1}\left(\frac{e\beta r_d}{2(k+1)}\right)^{-2(k+1)}, \end{aligned} \quad (88)$$

from which it can be shown that

$$\hat{\sigma}_k^2 \sim \frac{1}{8}\beta^2 \, \frac{1}{k} \, \frac{r_s^2}{r_d} \left(\frac{r_s}{r_d}\right)^{2k} \tag{89}$$

as $k \to \infty$.

Appendix C
SVD

In the presence of scatterers, we express the total field as the sum of the incident filed and the scattered field as in (27), where the scattered field (E_s, H_s) is set up by the currents J_s induced on the surface of the scattering objects. For the TM$_z$ polarization, the induced currents are in the z-direction. The scattered electric field is related to the surface current densities through

$$E_s(\mathbf{r}_d) = -\frac{\beta\eta}{4}\sum_{q=1}^{Q}\int_{\Gamma_q} J_q(\mathbf{r}_q) H_0^{(2)}\big(\beta|\mathbf{r}_d - \mathbf{r}_q|\big) d\gamma_q, \tag{90}$$

where Γ_q denotes the surface of the qth cylinder, $\mathbf{r}_q$ denotes a point on it, and $\mathbf{r}_d \in D$.

Since Γ_q is a conducting cylinder, we proceed by following similar steps as in [20] and express the coordinates of $\mathbf{r}_q \in \Gamma_q$ in terms of the local polar coordinates (a, ϕ_{qq}) with respect to the center of the qth cylinder and then expand the surface currents J_q in a Fourier series of the form

$$J_q(\mathbf{r}_q) = \frac{1}{2\pi a}\sum_{l=-\infty}^{\infty} K_l^{(q)} e^{jl\phi_{qq}}, \quad \mathbf{r}_q \in \Gamma_q. \tag{91}$$

where $K_l^{(q)}$ denotes the Fourier coefficient associated to the harmonic $e^{jl\phi_{qq}}$.

If the polar coordinates of the observation point $\mathbf{r}_d \in D$ with respect to the center of the qth cylinder are (r_{qd}, ϕ_{qd}), as depicted in Fig. 7, then by the addition theorem of Hankel functions

$$H_0^{(2)}\big(\beta|\mathbf{r}_d - \mathbf{r}_q|\big) = \sum_{m=-\infty}^{\infty} J_m(\beta a) e^{-jm\phi_{qq}} \times H_m^{(2)}(\beta r_{qd}) e^{jm\phi_{qd}}. \tag{92}$$

Substitution of (91) and (92) into (90) yields the electric field on the observation point with respect to the to the center of the qth cylinder

$$E_s(\mathbf{r}_d) = -\frac{\beta\eta}{4}\sum_{q=1}^{Q}\sum_{l=-\infty}^{\infty} K_l^{(q)} J_l(\beta a) H_l^{(2)}(\beta r_{qd}) e^{jl\phi_{qd}}. \tag{93}$$

To determine the Fourier coefficients $K_l^{(q)}$ in the current densities (91), we set up an electric field integral equation by requiring that the total field on the qth cylindrical surface be identically zero, i.e., $E(\mathbf{r}_q) = E_i(\mathbf{r}_q) + E_s(\mathbf{r}_q) = 0$ for all $\mathbf{r}_q \in \Gamma_q$. Following similar steps that lead to (93), we write

$$E_s(\mathbf{r}_q) = -\frac{\beta\eta}{4}\sum_{l=-\infty}^{\infty} K_l^{(q)} J_l(\beta a) H_l^{(2)}(\beta a) e^{jl\phi_{qq}} - \frac{\beta\eta}{4}\sum_{p\neq q}\sum_{l=-\infty}^{\infty} K_l^{(p)} J_l(\beta a) H_l^{(2)}(\beta r_{pq}) e^{jl\phi_{pq}}, \tag{94}$$

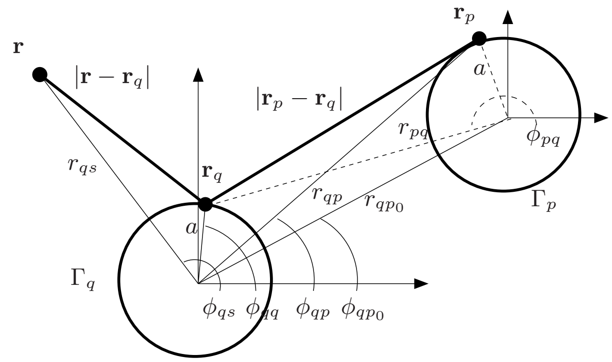

Fig. 7. Coordinate system with origin at the center of the qth cylinder .

where the pair (r_{pq}, ϕ_{pq}) denotes the polar coordinates of $\mathbf{r}_q$ with respect to the to the center of the pth cylinder (see Fig. (7)). By the addition theorem of the Hankel functions, observe that

$$H_l^{(2)}(\beta r_{pq}) e^{jl\phi_{pq}} = \sum_{m=-\infty}^{\infty} J_m(\beta a) e^{-jm\phi_{qq}} \times H_{m+l}^{(2)}(\beta r_{qp_0}) e^{j(m+l)\phi_{qp_0}}, \tag{95}$$

where (r_{qp_0}, ϕ_{qp_0}) denote the polar coordinates of the center of the pth cylinder with respect to the center of the qth cylinder.

Similarly, by combining (4) with (92), the incident field can be rewritten as

$$E_i(\mathbf{r}_q) = -\frac{\beta\eta}{4}\int_S I(\mathbf{r}) \sum_{m=-\infty}^{\infty} J_m(\beta a) e^{-jm\phi_{qq}} \times H_m^{(2)}(\beta r_{qs}) e^{jm\phi_{qs}} \, d\mathbf{r}, \tag{96}$$

where r_{qs} denotes the distance between $\mathbf{r}$ and the center of the qth cylinder and ϕ_{qs} is the polar angle of $\mathbf{r}$ with respect to the center of the qth cylinder.

After multiplying both sides of (94) and (96) by $e^{-jk\phi_{qq}}$, making use of (95), and integrating ϕ_{qq} over $[0, 2\pi]$, the boundary condition $E_s(\mathbf{r}_q) = -E_i(\mathbf{r}_q)$, $\mathbf{r}_q \in \Gamma_q$, yields the integral equation

$$K_k^{(q)} H_k^{(2)}(\beta a) + \sum_{p\neq q}\sum_{l=-\infty}^{\infty} K_l^{(p)} J_{-l}(\beta a) \times H_{l-k}^{(2)}(\beta r_{qp_0}) e^{j(l-k)\phi_{qp_0}} = -\int_S I(\mathbf{r}) H_k^{(2)}(\beta r_{qs}) e^{-jk\phi_{qs}} \, d\mathbf{r}. \tag{97}$$

A. Approximate Expression

Next, by Assumption 1 (Born approximation), the series of multiple scattering terms at the left hand side of (97) is assumed to be negligible. Then, an explicit solution for the unknowns Fourier series coefficients is possible:

$$K_k^{(q)} \approx -\frac{1}{H_k^{(2)}(\beta a)}\int_S I(\mathbf{r}) H_k^{(2)}(\beta r_{qs}) e^{-jk\phi_{qs}} \, d\mathbf{r}, \tag{98}$$

for every $q = 1, \ldots, Q$, and $k \in \mathbb{Z}$. Moreover, it follows from Assumption 2 (Point scatterers) that $\beta a << 1$, such that $|H_l^{(2)}(\beta a)| >> 0$ for all $l \neq 0$ and thus we can assume that in the Fourier series (91), $K_k^{(q)} \approx 0$ for all $k \neq 0$ and $q = 1, \ldots, Q$.

The only non-zero Fourier coefficient can be written as

$$\begin{aligned} K_0^{(q)} &\approx -\frac{1}{H_k^{(2)}(\beta a)} \int_S I(\mathbf{r}) H_0^{(2)}(\beta r_{qs})\, d\mathbf{r} \\ &= -\frac{1}{H_k^{(2)}(\beta a)} \int_S I(\mathbf{r}) \sum_{k=-\infty}^{+\infty} J_k(\beta r_s) \\ &\qquad \times H_k^{(2)}(\beta r_q) e^{jk(\phi_q - \phi_s)}\, d\mathbf{r} \\ &= -\frac{1}{H_k^{(2)}(\beta a)} \sum_{k=-\infty}^{+\infty} \langle I, J_k \rangle_S\, H_k^{(2)}(\beta r_q) e^{jk\phi_q}. \end{aligned}$$

Then, by resorting once again to the addition theorem and making use of the relationships $J_n(x) = (-1)^n J_{-n}(x)$ and $H_n^{(2)}(x) = (-1)^n H_{-n}^{(2)}(x)$, we write

$$H_0^{(2)}(\beta r_{qd}) = \sum_{m=-\infty}^{\infty} J_m(\beta r_d) H_m^{(2)}(\beta r_q) e^{m(\phi_d - \phi_q)}. \quad (99)$$

It follows that (93) can be approximated as

$$\begin{aligned} E_s(\mathbf{r}_d) &\approx -\frac{\eta\beta}{4} \sum_{q=1}^{Q} K_0^{(q)} J_0(\beta a) \\ &\quad \times \sum_{m=-\infty}^{\infty} J_m(\beta r_d) H_m^{(2)}(\beta r_q) e^{jm(\phi_d - \phi_q)} \\ &= \frac{\eta\beta}{4} \frac{J_0(\beta a)}{H_k^{(2)}(\beta a)} \sum_{q=1}^{Q} \sum_{k=-\infty}^{+\infty} \langle I, J_k \rangle_S H_k^{(2)}(\beta r_q) e^{jk\phi_q} \\ &\quad \times \sum_{m=-\infty}^{\infty} J_m(\beta r_d) H_m^{(2)}(\beta r_q) e^{jm(\phi_d - \phi_q)}. \quad (100) \end{aligned}$$

A similar approximate expression can be obtained for the magnetic field

$$\begin{aligned} H_s(\mathbf{r}_d) &\approx -j\frac{\eta}{4} \frac{J_0(\beta a)}{H_k^{(2)}(\beta a)} \sum_{q=1}^{Q} \sum_{k=-\infty}^{+\infty} \langle I, J_k \rangle_S\, H_k^{(2)}(\beta r_q) e^{jk\phi_q} \\ &\quad \times \sum_{m=-\infty}^{\infty} J_m'(\beta r_d) H_m^{(2)}(\beta r_q) e^{jm(\phi_d - \phi_q)}. \quad (101) \end{aligned}$$

In the following, we assume that (100) and (101) hold with equality.

B. The Average Scattered Field

Suppose that the scatterers are independently and uniformly distributed in the annular circle delimited by two concentric circles of radii r_d and $r_a > r_d$, of the same order of r_s. Then, averaging over ϕ_q yields

$$\begin{aligned} &\mathbb{E}\left(E_s(\mathbf{r}_d)\right) \\ &= \frac{1}{2\pi} \int_0^{2\pi} \frac{\eta\beta}{4} \frac{J_0(\beta a)}{H_0^{(2)}(\beta a)} \sum_{q=1}^{Q} \sum_{k=-\infty}^{+\infty} \langle I, J_k \rangle_S\, H_k^{(2)}(\beta r_q) \\ &\quad \times e^{jk\phi_q} \sum_{m=-\infty}^{\infty} J_m(\beta r_d) H_m^{(2)}(\beta r_q) e^{jm(\phi_d - \phi_q)}\, d\phi_q \\ &= \frac{\eta\beta}{4} \frac{J_0(\beta a)}{H_0^{(2)}(\beta a)} \sum_{q=1}^{Q} \sum_{k=-\infty}^{+\infty} \langle I, J_k \rangle_S \left(H_k^{(2)}(\beta r_q)\right)^2 \\ &\quad \times J_k(\beta r_d) e^{jk\phi_d}. \quad (102) \end{aligned}$$

By further averaging (102) in the radial direction we obtain

$$\begin{aligned} &\mathbb{E}\left(E_s(\mathbf{r}_d)\right) \\ &= \frac{\eta\beta}{4} \frac{J_0(\beta a)}{H_0^{(2)}(\beta a)} \sum_{k=-\infty}^{+\infty} \langle I, J_k \rangle_S\, \frac{2\pi Q}{\pi(r_a^2 - r_d^2)} \\ &\quad \int_{r_d}^{r_a} \left(H_k^{(2)}(\beta r)\right)^2 r dr\; J_k(\beta r_d) e^{jk\phi_d} \quad (103) \\ &= \frac{\eta\beta}{4} \sum_{k=-\infty}^{\infty} \|J_k(\beta r)\|_S\, \|w_k(\mathbf{r}_d)\|_D \\ &\quad \times \langle I, v_k \rangle_S\, \frac{w_k(\mathbf{r}_d)}{\|w_k(\mathbf{r}_d)\|_D}, \quad (104) \end{aligned}$$

where

$$\begin{aligned} w_k(\mathbf{r}_d) &= \frac{Q J_0(\beta a)}{H_0^{(2)}(\beta a)} \left(\frac{2\pi}{\pi(r_a^2 - r_d^2)} \int_{r_d}^{r_a} \left(H_k^{(2)}(\beta r)\right)^2 r dr \right) \\ &\quad \times J_k(\beta r_d) e^{jk\phi_d}. \end{aligned}$$

Similarly, the average magnetic field satisfies

$$\begin{aligned} \mathbb{E}\left(H_s(\mathbf{r})\right) &= -j\frac{\beta}{4} \frac{Q J_0(\beta a)}{H_0^{(2)}(\beta a)} \\ &\quad \times \sum_{k=-\infty}^{\infty} \left(\frac{2\pi}{\pi(r_a^2 - r_d^2)} \right. \\ &\quad \times \int_{r_d}^{r_a} \left(H_k^{(2)}(\beta r_q)\right)^2 r_q dr_q \|J_k'(\beta r)\|_S \\ &\quad \left. \times J_k'(\beta r_d) e^{jk\phi_d} \right) \langle I, v_k \rangle_S. \quad (105) \end{aligned}$$

Finally, it can be easily seen that equation (104) can be rewritten as (28) and (105) can be rewritten as (32).

C. Proof of Theorem 4 and 5

For fixed argument and large orders, we have

$$\begin{aligned} \sigma_k^{(s)} &\sim \frac{\eta\beta\, |\gamma_2|}{4\sqrt{\pi}}\, \frac{\sqrt{k+1}}{k^2(k^2-1)}\, \frac{r_s\, r_d^{5/2}}{r_a^2 - r_d^2} \left(\frac{r_s}{r_d}\right)^k \\ &\quad \times \left(1 - \left(\frac{r_d}{r_a}\right)^{2(k-1)}\right) \quad (106) \end{aligned}$$

and

$$\begin{aligned} \hat{\sigma}_k^{(s)} &\sim \frac{\eta\beta\, |\gamma_2|}{4\sqrt{\pi}}\, \frac{\sqrt{k+1}}{k(k^2-1)}\, \frac{r_s\, r_d^{3/2}}{r_a^2 - r_d^2} \left(\frac{r_s}{r_d}\right)^k \\ &\quad \times \left[1 - \left(\frac{r_d}{r_a}\right)^{2(k-1)}\right], \quad (107) \end{aligned}$$

from which the results follow.

REFERENCES

[1] C. E. Shannon, "A mathematical theory of communication," *Bell System Tech. J.*, vol. 27, pp. 379–423, 623–656, 1948.

[2] D. Gabor, *Light and information*, vol. 1. Amsterdam: Elsevier, 1961.

[3] G. Toraldo Di Francia, "Resolving power and information," *J. Opt. Soc. Amer.*, vol. 45, pp. 497–501, Jul. 1955.

[4] D. Slepian, "On bandwidth," *Proceedings of the IEEE*, vol. 64, pp. 292–300, Mar. 1976.

[5] O. M. Bucci and G. Franceschetti, "On the degrees of freedom of scattered fields," *IEEE Trans. Antennas Propagat.*, vol. 37, pp. 918–926, July 1989.

[6] O. M. Bucci and G. Franceschetti, "On the spatial bandwidth of scattered fields," *IEEE Trans. Antennas Propagat.*, vol. 35, pp. 1445–1455, Dec. 1987.

[7] İ. E. Telatar, "Capacity of multi-antenna Gaussian channels," *Europ. Trans. Telecommun.*, vol. 10, pp. 585–595, July 1999.

[8] O. Lévêque and İ. E. Telatar, "Information-theoretic upper bounds on the capacity of large extended ad hoc wireless networks," *IEEE Trans. Inf. Theory*, vol. 51, no. 3, pp. 858–865, 2005.

[9] D. A. B. Miller, "Communicating with waves between volumes: Evaluating orthogonal spatial channels and limits on coupling strengths," *Appl. Opt.*, vol. 39, pp. 1681–1699, Apr 2000.

[10] A. Poon, R. Brodersen, and D. Tse, "Degrees of freedom in multiple-antenna channels: A signal space approach," *IEEE Trans. Inf. Theory*, vol. 51, pp. 523–536, Feb. 2005.

[11] L. Hanlen and M. Fu, "Wireless communication systems with-spatial diversity: a volumetric model," *IEEE Trans. on Wireless Comm.*, vol. 5, pp. 133–142, Jan. 2006.

[12] M. Franceschetti, , and K. Chakraborty, "Space-time duality in multiple antenna channels," *IEEE Trans. on Wireless Communication*, 2007.

[13] M. D. Migliore, "On the role of the number of degrees of freedom of the field in MIMO channels," *IEEE Trans. Antennas Propagat.*, vol. 54, pp. 620–628, Feb. 2006.

[14] M. D. Migliore, "On electromagnetics and information theory," *IEEE Trans. Antennas Propagat.*, vol. 56, pp. 3188–3200, Oct. 2008.

[15] F. Gruber and E. Marengo, "New aspects of electromagnetic information theory for wireless and antenna systems," *IEEE Trans. Antennas Propagat.*, vol. 56, pp. 3470–3484, Nov. 2008.

[16] M. Jensen and J. Wallace, "Capacity of the continuous-space electromagnetic channel," *IEEE Trans. Antennas Propagat.*, vol. 56, pp. 524–531, Feb. 2008.

[17] M. Franceschetti, M. Migliore, and P. Minero, "The capacity of wireless networks: Information-theoretic and physical limits," *IEEE Trans. Inf. Theory*, vol. 55, pp. 3413 –3424, Aug. 2009.

[18] M. Franceschetti, M. Migliore, P. Minero, and F. Schettino, "The degrees of freedom of wireless networks via cut-set integrals," *IEEE Trans. Inf. Theory*, vol. 57, pp. 3067 –3079, May 2011.

[19] O. M. Bucci, C. Gennarelli, and C. Savarese, "Representation of electromagnetic fields over arbitrary surfaces by a finite and non redundant number of samples," *IEEE Trans. Antennas Propagat.*, vol. 46, pp. 351–359, Mar. 1998.

[20] R. Janaswamy, "On the EM degrees of freedom in scattering environments," *IEEE Trans. Antennas Propagat.*, vol. 59, pp. 3872–3881, Oct. 2011.

[21] A. Pinkus, *n-Widths in Approximation Theory*. Ergebnisse, Springer-Verlag, 1985.

[22] R. Kennedy, P. Sadeghi, T. Abhayapala, and H. Jones, "Intrinsic limits of dimensionality and richness in random multipath fields," *IEEE Trans. Signal Process.*, vol. 55, pp. 2542–2556, June 2007.

[23] A. Ishimaru, *Electromagnetic Wave Propagation, Radiation, and Scattering*. Prentice Hall, 1991.

[24] M. Abramowitz and I. A. Stegun, *Handbook of Mathematical Functions with Formulas, Graphs, and Mathematical Tables*. New York: Dover, 9th rd. ed., 1972.

[25] I. Gradshtein, I. Ryzhik, and A. Jeffrey, *Table of Integrals, Series, and Products*. A. Jeffrey, Editor, Academic Press., 1994.

[26] F. W. J. Olver, "The asymptotic expansion of bessel functions of large order," *Philos. Trans. Roy. Soc. London Ser. A*, vol. 247, pp. 328–368, 1954.

[27] F. W. J. Olver, "Tables for bessel functions of moderate or large orders," in *National Physical Laboratory Mathematical Tables*, London: Department of Scientific and Industrial Research, (Her Majesty's Stationery Office), vol 6., 1962.

[28] B. Hughes, *Asymptotics and special functions*. AKP Classics. A K Peters, Ltd., Wellesley, MA, 1997.